Available online at www.sciencedirect.com
ScienceDirect
Thin Solid Films 515 (2007) 3024–3029
thin solid films
www.elsevier.com/locate/tsf

Properties of transparent conducting oxides formed from CdO alloyed with In_2O_3

H.M. Ali *, H.A. Mohamed, M.M. Wakkad, M.F. Hasaneen

Physics Department, Faculty of Science, South Valley University, 82524 Sohag, Egypt

Received 20 April 2005; received in revised form 19 September 2005; accepted 29 June 2006
Available online 17 August 2006

Abstract

The structure, optical and electrical properties of transparent conducting oxide films depend greatly on the methods of preparation, heat treatment, type and level of dopant. Thin films of $(CdO)_{1-x}(In_2O_3)_x$ have been grown by electron beam evaporation technique for different concentrations of In_2O_3 (x=0, 0.05, 0.1, 0.15 and 0.2). Increase of doping led to increased carrier concentration as derived from optical data and hence to increased electrical conductivity, which degraded the transparency of the films. An improvement of the electrical and optical properties of Cadmium indium oxide ($CdIn_2O_4$) has been achieved by post-deposition annealing. A resistivity value of 7×10^{-5} Ω cm and transmittance of 92% in the near infrared region and 82% in the visible region have been obtained after annealing at 300 °C for 90 min in air.

Keywords: Structure properties; Transmittance; Optical energy gap; Resistivity; Carrier concentration; Mobility carriers

1. Introduction

Thin films of transparent conducting oxide (TCO) such as Zn, In, Sn, Cd oxides have received much attention because of their wide applications in the field of optoelectronic devices. Much more attention has been paid to study the electrical and optical properties of cadmium oxide (CdO) thin films, since they combine high optical transparency and high electrical conductivity, and therefore they are useful for various applications, such as solar cells [1–3], gas sensors [4], low-emissivity windows, wear resistant applications, flat panel displays, and thin-film resistors [5].

CdO is an n-type semiconductor, with a well-established direct band gap at approximately 2.5 eV [6]. When compared to ZnO, the transmittance of CdO in the visible region of the spectrum has been reported as rather low [7], however, cadmium oxide is characterized by a much lower resistivity.

Enhancing the electrical properties of TCOs, specially conductivity, can be done either by increasing the charge carrier concentration or by improving the mobility of those carriers. Increasing carrier concentration can be achieved by heavy doping of the TCO materials. This will, however, degrade the transparency due to increased free carrier absorption [8], and reduce the carrier mobility due to an increase in carrier scattering from ionized impurities. Increasing the mobility of charge carriers in TCOs will allow the conductivity to increase without compromising the transparency, thereby enhancing the overall performance of the TCO material.

The defect structures of oxides based upon CdO play a major role in determining their unique electrical and optical properties, which qualify them to serve as transparent conductors in a variety of well-known applications under specific conditions. Mixed oxides such as $CdO:In_2O_3$ have recently received considerable attention, since they combine many beneficial characteristics of both In_2O_3 and CdO. Undoped and doped CdO thin films have been obtained by different techniques such as reactive sputtering (RS) [9], sol–gel (SG) [10], and direct current reactive magnetron sputtering (DCRMS) [11], spray pyrolysis [12], and pulsed laser deposition (PLD) [5].

The aim of this study is to optimize the electrical and optical properties of indium-doped cadmium oxide thin films deposited by electron beam evaporation technique.

* Corresponding author.
E-mail address: hazem95@yahoo.com (H.M. Ali).

0040-6090/$ - see front matter © 2006 Elsevier B.V. All rights reserved.
doi:10.1016/j.tsf.2006.06.037

2. Experimental details

In our experiments $(CdO)_{1-x}(In_2O_3)_x$ (x=0, 0.05, 0.1, 0.15 and 0.2) films were prepared from highly pure (5 N) powders of CdO and In_2O_3 grinded separately and sieved. To insure complete mixing, these mixtures have been grinded together for 3 h. Then they have been made into tablet form using a cold pressing technique. In order to increase the diffusion process, the tablets were heated inside a furnace at 800 °C for 3 h. Thin films of the prepared $(CdO)_{1-x}(In_2O_3)_x$ tablet were deposited by electron beam evaporation technique onto ultrasonically cleaned microscopic glasses using Edwards high vacuum coating unit model E306A. The deposition conditions were: (1) a vacuum of 2.66×10^{-3} Pa (2×10^{-5} Torr), (2) an accelerating voltage of 3 kV, (3) electron beam current of 8–14 mA, and (4) the substrate temperature during deposition was maintained at room temperature. The film thickness (~150 nm) and deposition rate (10 nm/min) were controlled by means of a digital film thickness monitor model TM200 Maxtek. Post-deposition annealing temperature has been carried out in a fully controlled furnace in air for 15 min in the range from 150 to 550 °C. Annealing time has been noted also at 300 °C for different time of annealing. Structural analysis of as-deposited and annealed films was carried out on Phillips (PW-1710) *Cu-k_α* diffractometer (λ=1.541838 Å) by varying diffraction angle 2θ from 4 to 80 by step width of 0.04 in order to evaluate crystalline phase and crystallite orientation.

A Jasco V-570 UV–visible–NIR spectrophotometer was employed to record the transmission and reflection spectra over the wavelength range 200–2500 nm at normal incidence. The electrical resistivity was measured at room temperature using two-probe technique by means of a digital Keithley 614 electrometer.

Optical parameters namely, refractive index (n) and extinction coefficient (k), have been determined from the transmittance and reflectance measurements using the following relation [13,14]:

$$n=\frac{1+R}{1-R}\pm\left[\left(\frac{R+1}{R-1}\right)^2-\left(1+k^2\right)\right]^{1/2} \tag{1}$$

where $k=\frac{\alpha\lambda}{4\pi}$; α is the absorption coefficient.

Values of carrier concentration (N_{opt}) have been obtained using Drude's theory of dielectrics as follows.

The real dielectric constant (ε') can be written as [15,16]:

$$\varepsilon'=n^2-k^2=\varepsilon_i-\frac{e^2}{4\pi^2c^2\varepsilon_0}\left(\frac{N_{opt}}{m^*}\right)\lambda^2 \tag{2}$$

and,

$$\frac{e^2}{\pi c^2}\left(\frac{N_{opt}}{m^*}\right)\lambda^2=-4\pi\chi_c \tag{3}$$

where ε_i is the infinitely high frequency dielectric constant or the residual dielectric constant due to the ion core, N_{opt}/m^* is the ratio of carrier concentration to the effective mass, χ_c is the electric free carrier susceptibility and e is the elementary charge (1.6×10^{-19} C).

Values of the optical mobility (μ_{opt}) and resistivity (ρ_{opt}) were calculated using the following equations [17]:

$$\rho_{opt}=\frac{\tau}{\varepsilon_0\varepsilon_i\omega_P^2} \tag{4}$$

where ε_0 is the permittivity of free space and ω_P is the plasma frequency.

$$\text{and, } \mu_{opt}=\frac{1}{N_{opt}e\rho_{opt}} \tag{5}$$

3. Results and discussion

3.1. Film structure of as-deposited films

Fig. 1 shows the X-ray diffraction (XRD) patterns of as-deposited 150-nm-thick $(CdO)_{1-x}(In_2O_3)_x$ (x=0, 0.05, 0.1, 0.15 and 0.2) films. As it is seen for undoped film (x=0), three diffraction peaks associated with (111), (200) and (220) planes indicate that the film was polycrystalline in nature with cubic structure. For other compositions (x=0.05, 0.1, 0.15, and 0.2 wt.%), the observed diffraction peaks (311), (400) and (533) were at 32.36°, 39.01° and 66.99°, respectively indicating the formation of $CdIn_2O_4$. It has been observed also that the as-deposited films are blackish in color, which is due to the presence of free cadmium, indicated by the diffraction peak (110) at 62.45°. On the other hand, the intensities of crystalline phases of $(CdO)_{1-x}(In_2O_3)_x$ were found to be enhanced with increasing concentration of indium oxide ratio (x). The small shift in the positions of $CdIn_2O_4$ diffraction peaks is most likely due to a slight change in the lattice parameter associated with oxygen vacancies and In substitutes.

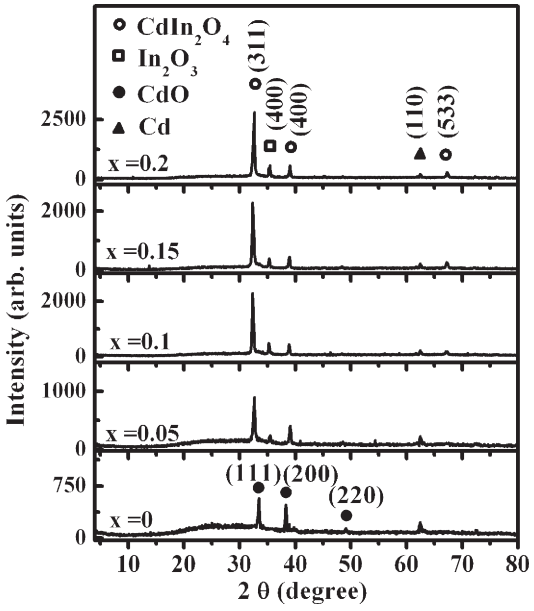

Fig. 1. X-ray diffraction patterns of as-deposited $(CdO)_{1-x}(In_2O_3)_x$ thin films, x=0, 0.05, 0.1, 0.15 and 0.2.

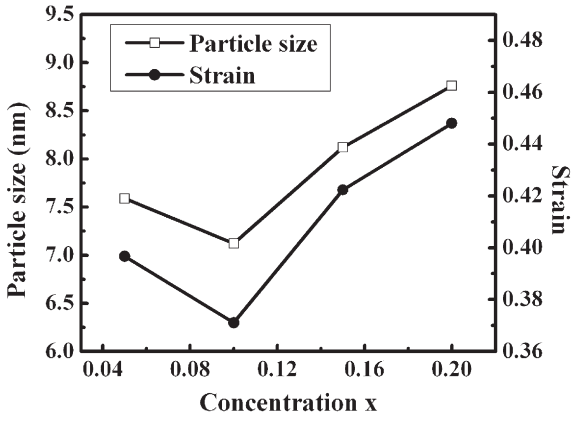

Fig. 2. Strain (ε) and particle size (D) along the [311] direction of the as-deposited $(CdO)_{1-x}(In_2O_3)_x$ thin films, $x=0$, 0.05, 0.1, 0.15 and 0.2.

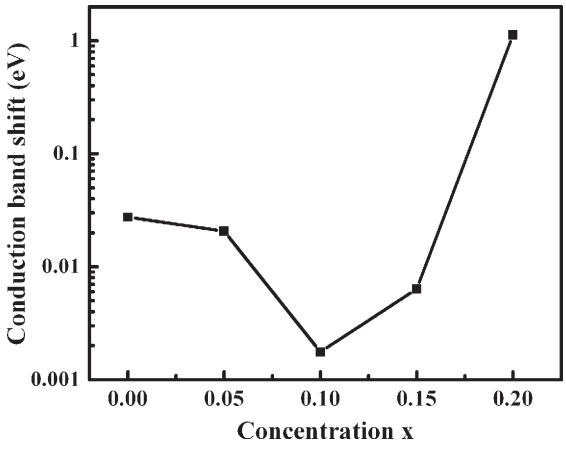

Fig. 4. Plot of the conduction band shift of as-deposited $(CdO)_{1-x}(In_2O_3)_x$ as a function of In_2O_3 content.

The structural parameters of the films have been calculated from the XRD patterns depicted in Fig. 1. One can show that the preferential growth is along the [311] direction, other peaks associated to the preferential one appear, but their intensity is less important than (311) plane. The strain (ε) and particle size (D) of as-deposited $(CdO)_{1-x}(In_2O_3)_x$ films have been obtained from the following relation [18]:

$$\frac{\beta\cos\theta}{\lambda}=\frac{1}{D}+\frac{\varepsilon\sin\theta}{\lambda}$$

where β is the full-width at half-maximum of the diffraction peak. From the plot of $(\beta\cos\theta)/\lambda$ versus $(\sin\theta)/\lambda$, the values of slope and intercept yield the strain and particle size respectively, whose results are plotted in Fig. 2.

3.1.1. Optical and electrical properties of as-deposited films

Fig. 3 depicts the transmittance (T%) spectra of 150-nm-thick as-deposited indium-doped cadmium oxide films for different concentration of indium oxide x in the wavelength range from 200 to 2500 nm. In the inset of Fig. 3, the average transmittance in the visible (T_{vis}) and infrared (T_{IR}) regions is shown. The transmittance of cadmium indium oxide is expected to depend mainly on three factors: (1) oxygen deficiency, (2) surface roughness (surface scattering reduces the transmission, which in turn depends on the particle size), and (3) impurity centers. It is observable that all films show poor optical transmittance either in visible or near infrared regions, which can be attributed to the oxygen deficiency [19]. It is evident also that the transmittance except at $x=0.1$ decreased with increasing indium oxide content x, whereas at high carrier concentrations the crystal are modified because of carrier–carrier interaction and carrier–impurity interaction, which can lead to a narrowing of the band gap. However, high carrier concentrations also lead to larger free carrier absorption [8] and at the same time, it lowers the mobility due to more charge carrier scatterings from ionized impurities.

According to Wolff [20] at high carrier concentrations, the conduction band is shifted downward by a quantity equal to $E^{EX}=(q/2\pi\varepsilon_0\varepsilon_r)(3N/\pi)^{1/3}$, where q is the electron charge, ε_0 is the permittivity of vacuum, and ε_r is the dielectric constant. Fig. 4 shows the conduction band shift as a function of composition. It is obvious that the film with $x=0.1$ has the lowest shift or has the highest energy gap as compared with other compositions in the present work.

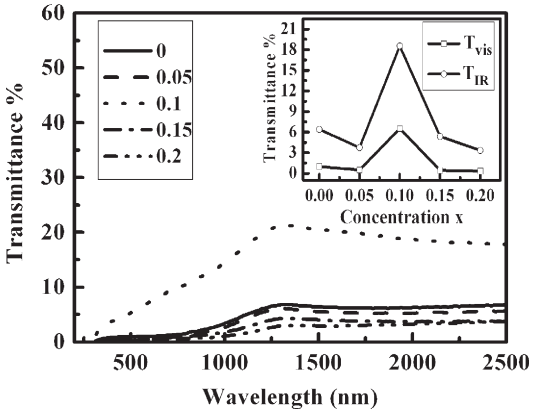

Fig. 3. Transmittance spectra of as-deposited $(CdO)_{1-x}(In_2O_3)_x$ films $x=0$, 0.05, 0.1, 0.15 and 0.2. In the inset the average transmittance in the visible (T_{vis}) and infrared (T_{IR}) regions is shown.

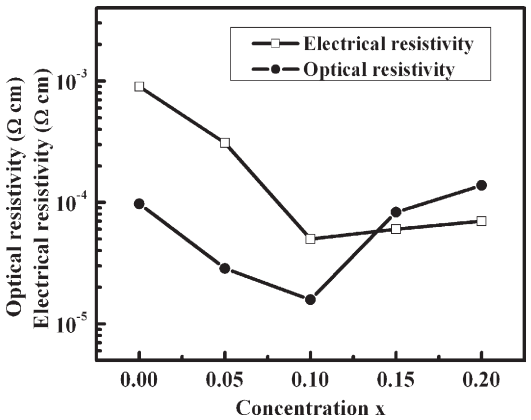

Fig. 5. Variation of the electrical and optical resistivities ρ of the as-deposited $(CdO)_{1-x}(In_2O_3)_x$ films with In_2O_3 content.

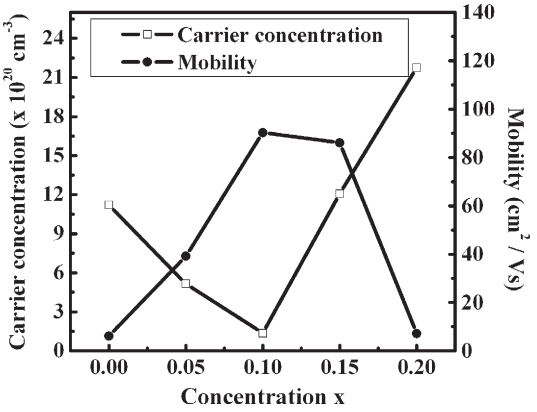

Fig. 6. Plot of the free carrier concentration and mobility carriers calculated from the optical data for as-deposited $(CdO)_{1-x}(In_2O_3)_x$ films as a function of In_2O_3 content.

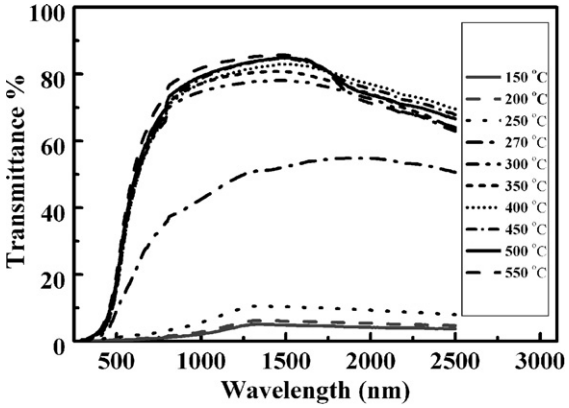

Fig. 8. Typical data of spectral normal transmittance of $(CdO)_{0.9}(In_2O_3)_{0.1}$ films annealed at different temperatures for 15 min.

Fig. 5 shows the electrical and optical resistivity ρ of the as-deposited films. It is clear that both the electrical and optical resistivity decreased with increasing In_2O_3 content, reached a minimum value of 5×10^{-5} Ω cm for the electrical resistivity and of 1.57×10^{-5} Ω cm for calculated optical resistivity at $x=0.1$, then the resistivity increased above $x=0.1$. As explained before, the structural quality of the films increases with increasing concentration x. Therefore, the initial decrease in the film resistivity can be explained as very likely due to the carrier concentration and electron mobility, which have been calculated optically using Eqs. (3) and (5) respectively. As seen in Fig. 6, with increasing x the mobility of the films increased from 6 to 91 cm^2/V s and the carrier concentration decreased from 1.12×10^{21} to 1.37×10^{20} cm^{-3} for $x=0.1$, then the mobility decreased to 7.17 cm^2/V s and the carrier concentration increased. So, the increase of the resistivity (either measured electrically or calculated optically) above $x=0.1$ can be attributed to the concentration of indium impurity higher than the optimum value and to the decrease of mobility carriers.

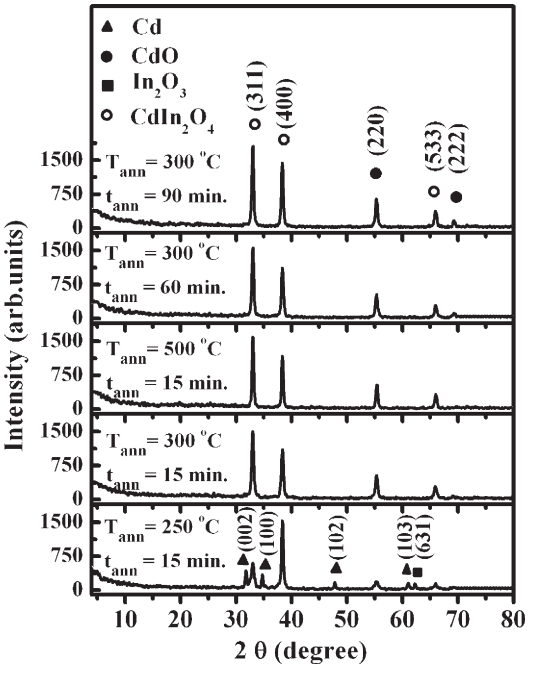

Fig. 7. X-ray diffraction patterns of $(CdO)_{1-x}(In_2O_3)_x$ films with $x=0.1$ annealed at different temperatures and times.

3.2. Effect of annealing temperature

3.2.1. Film structure

The effect of annealing temperature and time on the structural properties of $(CdO)_{1-x}(In_2O_3)_x$ film with $x=0.1$ is shown in Fig. 7. The diffraction patterns indicate that the films are polycrystalline in nature with cubic structure. It is clear that the intensities of crystalline phases of $CdIn_2O_4$ and CdO were found to be enhanced with increasing annealing temperature and time. On the other hand, the full-width at half-maximum (FWHM) decreases with increasing temperature of annealing, indicating the increase of the grain size with increasing annealing temperature. Upon annealing at 250 °C, all atoms of Cd are completely oxidized and In_2O_3 peaks are not found, which implies that indium atoms replace cadmium in the lattice or indium segregates to the non-crystalline regions in grain boundaries.

3.2.2. Optical and electrical properties

As mentioned before, enhancing the conductivity of TCOs can be done either by increasing the charge carrier concentration

Table 1
Variations of the electrical resistivity ρ, of the mobility carriers μ and the free carriers concentration N calculated from the optical data, and of optical band gap E_g of $(CdO)_{0.9}(In_2O_3)_{0.1}$ with different annealing temperatures

T_{ann} (°C)	ρ (Ω cm)	μ (cm^2/V s)	N (cm^{-3})	E_g (eV)
150	6×10^{-5}	47.49	2.19×10^{21}	2.03
200	3.4×10^{-4}	12.36	1.48×10^{21}	2.15
250	3.3×10^{-4}	18.46	1.02×10^{21}	2.26
270	3.31×10^{-4}	23.45	8.04×10^{20}	2.5
300	2.0×10^{-4}	230.22	1.35×10^{20}	2.71
350	1.1×10^{-3}	54.02	1.1×10^{20}	2.69
400	8.2×10^{-4}	192.5	3.95×10^{19}	2.64
450	5.95×10^{-4}	184.85	5.72×10^{19}	2.71
500	5.92×10^{-4}	114.32	9.25×10^{19}	2.65
550	5.90×10^{-4}	101.06	1.05×10^{20}	2.7

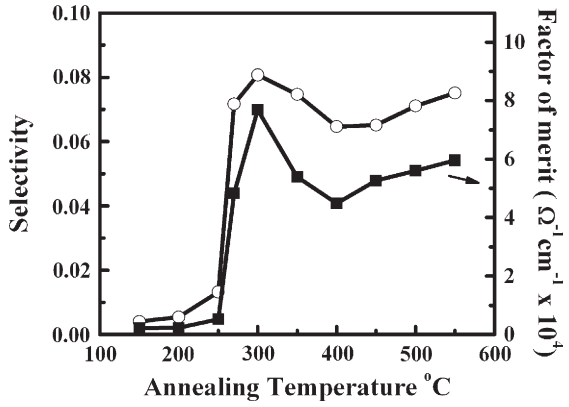

Fig. 9. Annealing temperature dependence of the factor of merit and selectivity for $(CdO)_{0.9}(In_2O_3)_{0.1}$ films.

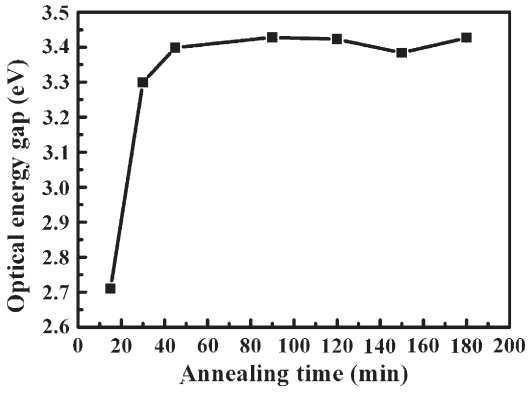

Fig. 11. Variation of the optical band gap E_g of $(CdO)_{0.9}(In_2O_3)_{0.1}$ film with annealing time at 300 °C.

or by improving the mobility of those carriers. However increasing carrier concentration may degrade the transparency due to increased free carrier absorption [8]. In that context, post-deposition annealing has been noted to be helpful in improving the film's electro-optical properties [14,21]. As-deposited films with $x=0.1$ have been annealed at different temperatures in the range from 150 to 550 °C for 15 min. Fig. 8 illustrates the optical transmittance of the annealed films. It is seen that the transmission improved significantly after annealing due to an apparent shift in the absorption edge to lower wavelength value. For film annealed for 15 min at temperature of 300 °C or higher, the average transmission in the visible region has increased to around 34%.

Table 1 presents the electrical and optical properties of $(CdO)_{0.9}(In_2O_3)_{0.1}$ annealed at different temperatures. The resistivity was in the range of $0.6–8.5\times10^{-4}$ Ω cm. The mobility carriers as estimated from optical measurements was in the range 12.36–230.22 cm^2/V s and attains the maximum value at $T_{ann}=300$ °C while the carrier concentration decreases with increasing annealing temperature. Using the optical absorption coefficient α evaluated from the optical transmission data, the allowed direct band gap E_g values were obtained by extrapolating the linear portion of the plots of $(\alpha h\nu)^2$ versus $h\nu$ to $\alpha=0$. The change in the optical band gap is relatively small for films annealed at different temperatures, and is in the range of 2.03–2.71 eV. The increase of optical band gap with increasing annealing temperature may be due to the decrease of carrier concentration.

To judge the quality of the film as a selective transmission layer in the visible region, Carl et al. [22], have used the following expression for selectivity, $S=T_{vis}(1-T_{IR})$. The figure of merit $\varphi=T/\rho$ [23] was also used to evaluate the quality of a film as transparent-conductive material. Fig. 9 shows the annealing

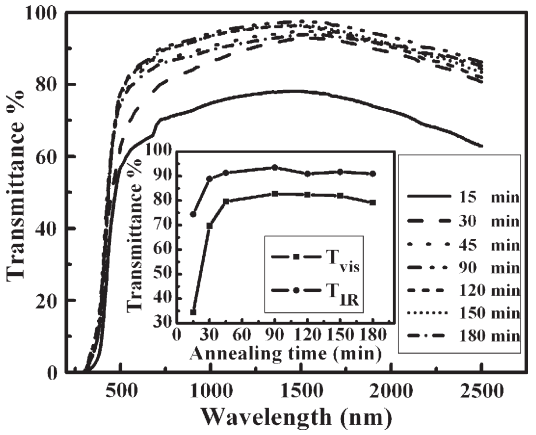

Fig. 10. Spectral variation of the transmittance T% with wavelength of $(CdO)_{0.9}(In_2O_3)_{0.1}$ film for different annealing times at 300 °C. In the inset variation of the average transmittance in the visible (T_{vis}) and infrared (T_{IR}) regions with annealing time is shown.

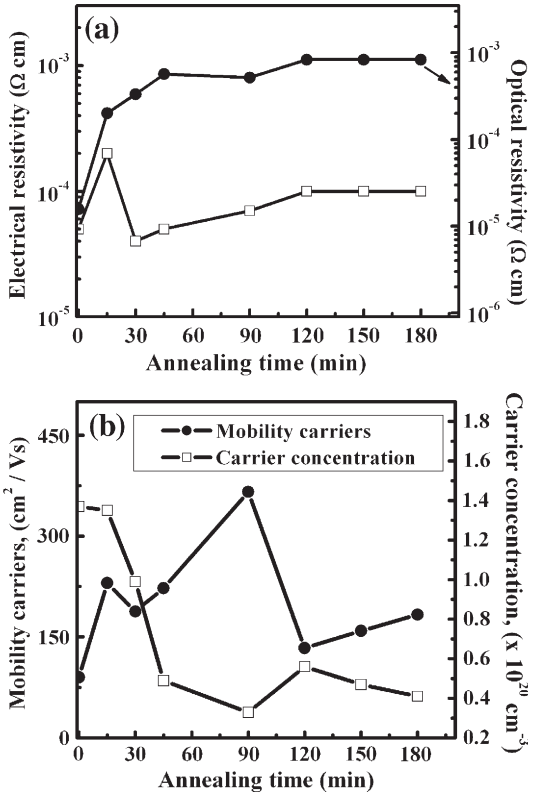

Fig. 12. Plot of (a) the electrical and optical resistivities; and (b) the mobility carriers and the free carrier concentration calculated from the optical data for $(CdO)_{0.9}(In_2O_3)_{0.1}$ thin film annealed at 300 °C as a function of annealing time.

temperature dependence of the factor of merit and selectivity for $(CdO)_{0.9}(In_2O_3)_{0.1}$ films. The selectivity has reached more than 0.065 and the figure of merit has increased to $>5\times10^4\ \Omega^{-1}\ cm^{-1}$ when samples were annealed at $T_{ann}\geq275$ °C for 15 min. The maximum values of both the selectivity and the figure of merit have been achieved at $T_{ann}=300$ °C.

3.3. Effect of annealing time

3.3.1. Optical and electrical properties

To improve electro-optical properties of $(CdO)_{1-x}(In_2O_3)_x$ film with $x=0.1$, annealing has been performed at 300 °C for different times. The wavelength dependence of transmission spectra of $(CdO)_{0.9}(In_2O_3)_{0.1}$ annealed at 300 °C for different times of annealing is shown in Fig. 10. It is clear that the transmission improved significantly with increasing time of annealing and goes up to 82% in the visible region and up to 92% in the NIR region. High transmittance in the visible region of the spectrum suggests the possible use of these films as glazing materials.

The dependence of optical band gap on time of annealing is shown in Fig. 11. The optical band gap of the films increased from 2.71 eV to 3.35 eV with an increase in the time of annealing from 15 to 30 min. This indicates that annealing in air at 300 °C for 30 min is an effective means for enhancing the optical transmittance. The optical band gap increases further with increasing time of annealing to reach its maximum value of 3.43 eV for film annealed at 300 °C for 90 min. The increase of optical band gap with increasing annealing time may be due to the decrease of carrier concentration [24].

The electrical and optical resistivity, carrier concentration and the mobility carriers of $(CdO)_{0.9}(In_2O_3)_{0.1}$ annealed at 300 °C as a function of annealing time are shown in Fig. 12. The low values of the optical resistivity are due to the high values of mobility carriers. The electrical resistivity of the film annealed at 300 °C for 15 min was $2\times10^{-4}\ \Omega$ cm. It initially decreased to $4\times10^{-5}\ \Omega$ cm with increasing time of annealing for 30 min, which compares favorably with resistivity value for as-deposited film of $5\times10^{-5}\ \Omega$ cm and afterwards increased slightly to reach its maximum value of $1\times10^{-4}\ \Omega$ cm for further increase of the time of annealing. The initial decrease in the electrical resistivity indicated an optimum requirement of the time of annealing to prepare low resistive $CdIn_2O_4$ films. The increase in the film resistivity with annealing temperature can be attributed to the incorporation of oxygen atoms (due to heat in air) which can cause a decrease in current carriers and hence an increase in resistivity [21]. On the other hand, the optical resistivity (2×10^{-4}–$8\times10^{-4}\ \Omega$ cm) is slightly higher than the measured one, but it shows the same tendency.

4. Conclusions

Indium-doped cadmium oxide films were deposited on glass substrates using electron beam evaporation technique. Structural, optical, and electrical properties have been studied. X-ray diffraction study showed that indium-doped cadmium oxide films were polycrystalline with preferred orientation along (311), (400), (533) planes. It was also observed that, for as-deposited films, the increase of carrier concentration led to a degradation of the transparency due to increased free carrier absorption, and to a decrease of the carrier mobility. Increasing the mobility of charge carriers in the TCOs allowed the conductivity to increase without compromising the transparency, thereby enhancing the overall performance of the TCO material. Post-deposition annealing has been noted to be helpful in improving the electro-optical properties of the films. An average transmittance value of 92% in the NIR region and 82% in the visible region of the spectrum and a resistivity of $7\times10^{-5}\ \Omega$ cm were obtained for $(CdO)_{1-x}(In_2O_3)_x$ film with $x=0.1$ annealed at 300 °C for 90 min. The fabricated film exhibited a high optical band gap of 3.43 eV corresponding to a direct band gap transition.

References

[1] C. Champness, C. Chan, Sol. Energy Mater. Sol. Cells 37 (1995) 75.
[2] C. Sravani, K. Ramakrishna, O. Hussain, P. Reddy, J. Sol. Energy Soc. India 6 (1996) 1.
[3] O. Vigil, L. Vaillant, F. Cruz, G. Santana, A. Morales-Acevedoc, G. Contreras-Puente, Thin Solid Films 361–362 (2000) 53.
[4] A. Shiori, Jpn. Patent 7,909, (1979) 995.
[5] E. Martin, M. Yan, M. Lane, J. Ireland, C. Kannewurf, R.H. Chang, Thin Solid Films 461 (2004) 309.
[6] D. Carballeda-Galicia, R. Castanedo-Pérez, O. Jiménez-Sandoval, S. Jiménez-Sandoval, G. Torres-Delgado, C. Zúñiga-Romero, Thin Solid Films 371 (2000) 105.
[7] Y. Choi, C. Lee, S. Cho, Thin Solid Films 289 (1996) 153.
[8] H. Kim, J. Horwitz, W. Kim, A. Makinen, Z. Kafafi, D. Chrisey, Thin Solid Films 420–421 (2002) 539.
[9] T. Lakshmanan, J. Electrochem. Soc. 110 (1963) 548.
[10] J. Santos-Cruz, G. Torres-Delgado, R. Castanedo-Perez, S. Jiménez-Sandoval, O. Jiménez-Sandoval, C.I. Zúñiga-Romero, J. Marquez Marín, O. Zelaya-Angel, Thin Solid Films 493 (2005) 83.
[11] K. Gurumurugan, D. Mangalaraj, Sa. K. Narayandass, J. Electron. Mater. 25 (1996) 765.
[12] R. Ferro, J.A. Rodriguez, Thin Solid Films 347 (1999) 295.
[13] J. Tauc, in: J. Tauc (Ed.), Amorphous and Liquid Semiconductors, Plenum Press, New York, 1979, p. 159.
[14] E. Shokr, M. Wakkad, H. Abd El-Ghanny, H. Ali, Eur. Phys. J. Appl. Phys. 8 (1999) 215.
[15] W.G. Spitzer, H.Y. Fan, Phys. Rev. 106 (1957) 882.
[16] E. Kh. Shokr, M.M. Wakkad, H.A. Abd El-Ghanny, H.M. Ali, J. Phys. Chem. Solids 61 (2000) 75.
[17] H. Haitjema, J.J. Ph. Elich, Thin Solid Films 205 (1991) 93.
[18] S. Quadri, E. Skelton, D. Hsu, A. Dinsmore, J. Yang, H. Gray, B. Ratna, Phys. Rev., B 60 (1999) 9191.
[19] K. Tanaka, A. Kunioka, Y. Sakai, Jpn. J. Appl. Phys. 8 (1969) 681.
[20] P. Wolff, Phys. Rev. 126 (1962) 405.
[21] H.M. Ali, H.A. Mohamed, S.H. Mohamed, Eur. Phys. J. Appl. Phys. 31 (2005) 87.
[22] K. Carl, H. Schmitt, I. Friedrich, Thin Solid Films 295 (1997) 151.
[23] C. Terrier, J. Chatelon, J. Roger, Thin Solid Films 295 (1997) 95.
[24] K. Gurumuragan, D. Mangalaraj, Sa. K. Narayandas, C. Bala-subramanyan, Phys. Status Solidi, A Appl. Res. 143 (1994) 85.